IJST, Transactions of Mechanical Engineering, Vol. 37, No. M2, pp 189-202
Printed in The Islamic Republic of Iran, 2013


# OPTIMIZATION OF DIE PROFILE FOR COLD FORWARD EXTRUSION USING AN IMPROVED SLAB METHOD ANALYSIS*

F. GHAEMI, R. EBRAHIMI** AND R. HOSSEINIFAR

Dept. of Materials Science and Engineering, School of Engineering, Shiraz University, Shiraz, I. R. of Iran
Email: ebrahimy@shirazu.ac.ir

**Abstract–** One of the most important design parameters in extrusion process is the shape of die profile. In the present research work, an optimum extrusion die profile has been obtained through implementation of slab analysis in a computational algorithm. Moreover, extrusion process through both optimum conical and curved die has been performed experimentally and also by finite element method. It has been demonstrated that material work hardening characteristics and friction condition have remarkable effects on the optimum streamlined die profile. Also, results prove that the streamlined die profile designed based on the developed approach, is superior to the conventional conical dies from both metallurgical and manufacturing perspectives. Consequently, the proposed method can be regarded as an efficient and reliable tool for designing streamlined die profiles. Hence, this technique can be used to produce desirable conditions in both process and product quality in terms of extrusion force, deformation homogeneity and die wear.

**Keywords–** Extrusion, die profile, finite element analysis, slab method, strain distribution

## 1. INTRODUCTION

Economic requirements and development of new alloys have compelled the manufacturing industries to modify their conventional manufacturing technology. The extrusion technology is not an exception to this rule and needs essential changes. One of these changes is modification of the geometrical shape of extrusion die profile. Die profile has a considerable effect on metal flow characteristics, final product microstructure, productivity and die life.

Conventionally, the extrusion process is carried out using either flat face or conical dies. In these dies the flowing material is subjected to abrupt changes in velocity and cross section. Hence, they suffer from many drawbacks such as formation of dead metal zone, more redundant work and therefore need higher capacity presses. However, it is possible to overcome these problems by using an optimal design. Furthermore, the level of die wear can be minimized and therefore longer die life can be achieved. In the past, due to the difficulty of manufacturing curved dies, conical dies were the preferred choice. Nevertheless, nowadays with the advent of computer numerical control (CNC) machines, and hence, the ease of manufacturing of complex die shapes, many researchers have become motivated to develop various techniques to design curved die profiles for the forward rod extrusion process.

A breakthrough in the die design methodology occurred in the work of Richmond and Devenpeck [1]. They designed ideal plane strain dies using slip-line theory under the assumption of no work hardening material and frictionless die that produced no redundant strain. Their results triggered interest in an investigation into introducing new die types for metal extrusion, and justification for research in relation to extrusion die design. Srinivasan *et al.*[2] using slab method analysis proposed a controlled

*Received by the editors February 27, 2013; Accepted May 20, 2013.
**Corresponding author

strain rate die with a streamlined shape which improved the extrusion process for materials with limited workability. Then, Lu and Lo [3] used a refined slab method to account for friction and material property changes in the deformation zone. Jooybari *et al.* [4] proposed a new combined slab method and upper bound technique to obtain the deformation load in forward rod extrusion. Their analytical, numerical and experimental results illustrate that the required load in the optimum curved die during the deformation is significantly less than that in the optimum conical die.

Many researchers used finite element method (FEM) to obtain optimum die profile. Byon and Hwang [5] applied a FEM-based optimal process design technique in both cold and hot extrusion to die profile design in forward extrusion and found that strain hardening and heat transfer affect the optimal die profile markedly. Lin *et al.* [6] have used a 12-interval cubic spline curve to design an optimized hot extrusion die with FEM to minimize wear. They varied the die surface so as to obtain a uniform distribution of load. Kim *et al.* [7] optimized die profile of axisymmetric extrusion of metal matrix composites using FEM in order to obtain uniform strain rate profile.

Several attempts have been made to design die profile using upper bound theory. Gordon *et al.*[8-10] used a new optimized velocity field to determine an adaptable die shape which minimized the extrusion pressure. They found that their proposed die profile is superior to the streamlined die shape of Yang and Han [11]. Ponalagusamy *et al.*[12] designed streamlined dies based on Bezier curves and polynomial equations using upper bound method and compared them with each other. Bezier curve dies were found to take lower extrusion pressure. Pahlavani and Ebrahimi [13] investigated three different die profiles for tube extrusion by upper bound theory and FEM. They found that the cosine profile offers the best energy wise efficiency while the CRHS profile is the best profile from the aspect of strain homogeneity.

In spite of numerous investigations conducted on the extrusion die design, very few attempts [5] have been made to evaluate the effect of workpiece material properties on the optimum die profile, which is of crucial importance in results accuracy. The aim of the present work is to introduce a simple and yet reliable method in tool design in forward extrusion process by utilizing a computational algorithm. Wifi et al. [14] and Noorany Azad et al. [15] have done such a work for hot extrusion of steel and cold extrusion of aluminum respectively. They obtained a second order die profile curve which is not smooth enough. However, in the current work, the governing differential equation, the used algorithm and the method of quantitative assessment of redundant work are ameliorated and therefore a vastly superior die profile was obtained. Indeed, the main merit of the proposed approach, apart from its simplicity, efficiency and capability to deal with various processes and material variables, is shown by the fact that the effect of material work hardening can be thoroughly reflected. Validity of the proposed approach was demonstrated via conducting experiments and FE simulation on the extrusion of aluminum through the designed curved die and conical die. In order to study the deformation homogeneity in extruded products Vickers microhardness test was used. In addition, to evaluate the wear behavior of dies, Archard wear model was employed.

## 2. DESIGN PROCEDURE OF OPTIMAL DIE PROFILE

### *a) Incremental slab method*

In order to estimate the extrusion pressure in a curved die, incremental slab method presented by Wifi *et al.* [14] was used. In this method, deformation zone is compartmentalized to a specified number of slabs, each of which can be considered as a small conical die. By analyzing each slab individually, the required pressure to extrude the billet through curved die can be obtained. In other words, slab method of analysis is reformulated in an incremental form. The detailed analysis is presented further on. It is worth

mentioning that in cold extrusion processes, temperature variation in workpiece is negligible and this obviates the need for heat transfer analysis.

***b) Extrusion pressure in each slab***

Extrusion pressure equation in each slab can be derived by making a force balance on a differentially thick "*spherical*" slab of material at deformation zone (Fig. 1). It should be mentioned that the curved surfaces of this slab are geometrically spherical. Panteghini and Genna [16] have derived the average drawing stress for wire drawing process by using this type of slab. In the present work by applying appropriate boundary conditions for extrusion process, differential equation obtained from force balance on this slab is solved and an equation for estimation of extrusion pressure in each slab is derived. Using this type of slab for calculating extrusion pressure would eliminate the need to use simplified assumption, which may lead to error accumulation in results. In the case of using "plane slab" originally developed by Sachs [17], inevitably it is assumed that the created shear stress on the slab surface will not provide any change in the principal stress directions [18]. It is crucial to realize that this assumption becomes unrealistic and progressively worse in high semi-die angles and high friction coefficients.

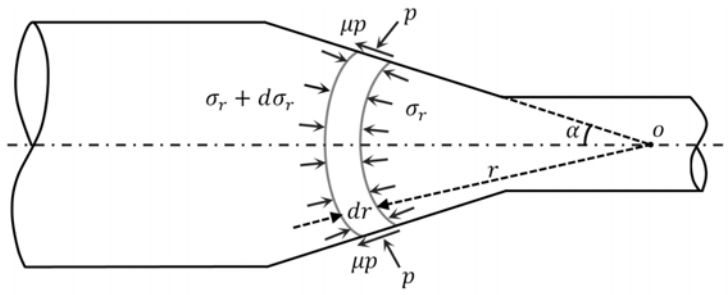


Fig. 1. Schematic illustration of the spherical slab and stress field around it

To consider the effect of material work hardening in slab analysis, a linear work hardening relation is used. Integrating this relation in solving the differential equation derived from the force balance would then enable one to calculate the flow stress of material in any point and avoid the errors caused by taking a constant or mean flow stress. Other mathematical expressions for the flow curve can result in considerable mathematical complexity when they are used with the force balance equation and can be a hindrance solving the equation analytically. It is worth noting that the assumption of linear work hardening in this analysis is not far from reality, since in the situations of imposing rather large compressive strains, material work hardening exhibits a linear behavior instead of having power-law variations [19, 20]. The mentioned behavior is given by the following equation:

$$\sigma_y = \sigma_0 + h\varepsilon \tag{1}$$

where $h$ and $\sigma_0$ denote slope and ordinate of the line which passes through the pseudo-linear part of true stress-strain curve respectively. $\varepsilon$ is the current true strain and can be calculated in spherical coordinate system as follows:

$$\varepsilon = 2\ln\frac{r_0}{r} \tag{2}$$

in which $r_0$ is the radial distance between die entrance and die apex and *r* is current radial distance of each point in deformation zone from die apex. It should be noticed that *r* varies from $r_0$ to $r_f$ (Fig. 1).

Summing all the corresponding component of forces in the *x*-direction (extrusion direction) over the above-mentioned spherical slab results in

$$\sigma_r(2rdr)\int_0^{\alpha}\sin\theta\cos\theta d\theta + d\sigma_r(r^2+2rdr)\int_0^{\alpha}\sin\theta\cos\theta d\theta + pr\sin^2\alpha dr + \mu p\sin\alpha\cos\alpha rdr = 0 \tag{3}$$

where $\alpha$ is the semi-die angle, $\theta$ is the current angle of each point in deformation zone which measures from symmetrical axis, $\mu$ is the coefficient of friction between die and workpiece, $\sigma_r$ is the radial stress and $p$ is the pressure normal to the die. After some passages and simplifying, Eq. (3) becomes:

$$2\sigma_r dr + rd\sigma_r + 2pdr + 2\mu p\cot\alpha dr = 0 \tag{4}$$

To solve Eq. (4), the relation between $p$ and $\sigma_r$ must be found and substituted. Considering von Mises yield criterion and spherical symmetry in problem, one can write:

$$p = \sigma_y - \sigma_r \tag{5}$$

where $\sigma_y$ is given by Eq. (1).

Combining Eqs. (4) and (5), and solving the resulted differential equation, one obtains:

$$\sigma_r = \frac{C}{r^{2-\beta}} + \frac{\beta\left(2h\ln\frac{r_0}{r}+\sigma_0\right)}{\beta-2} - \frac{2\beta h}{(\beta-2)^2} \tag{6}$$

in which $\beta = 2(1+\mu\cot\alpha)$ and $C$ is integral constant which is related to the boundary condition. Eq. (6) expresses the extrusion pressure in each slab radially. Therefore, in order to represent it in a horizontal manner, horizontal projection of radial stress on exit and entrance surfaces of die must be averaged as follows:

$$\sigma_{xf} = \frac{1}{\pi(r_f\sin\alpha)^2}\int_0^{\alpha} 2\pi r_f{}^2\sigma_r(r=r_f)\cos\theta\sin\theta d\theta = \sigma_r(r=r_f) = \sigma_{rf} \tag{7}$$

and similarly for entrance surface:

$$\sigma_{xb} = \frac{1}{\pi(r_0\sin\alpha)^2}\int_0^{\alpha} 2\pi r_0{}^2\sigma_r(r=r_0)\cos\theta\sin\theta d\theta = \sigma_r(r=r_0) = \sigma_{rb} \tag{8}$$

By applying appropriate boundary condition at the die exit i.e. $\sigma_r = \sigma_{rf}$ at $r = r_f$, into Eq. (6) and using Eq. (7), the radial extrusion pressure is obtained as:

$$\sigma_r = \frac{\left[\sigma_{xf} - \frac{\beta(\beta-2)\left[(2h\ln\frac{r_0}{r_f}+\sigma_0)\right]-2\beta h}{4-4\beta+\beta^2}\right] r_f{}^{2-\beta}}{r^{2-\beta}} + \frac{\beta\left[(\beta-2)\left(2h\ln\frac{r_0}{r}+\sigma_0\right)-2h\right]}{4-4\beta+\beta^2} \tag{9}$$

Similarly at the die inlet, applying boundary condition $\sigma_r = \sigma_{rb}$ at $r = r_0$ into Eq. 9 and using Eq. (8) one can finally obtain:

$$\sigma_{xb}=\frac{\left[\sigma_{xf}-\frac{\beta(\beta-2)\left[(2h\ln\frac{r_0}{r_f}+\sigma_0)-2\beta h\right]}{4-4\beta+\beta^2}\right]r_f^{2-\beta}}{r_0^{2-\beta}}+\frac{\beta[\sigma_0(\beta-2)-2h]}{4-4\beta+\beta^2} \tag{10}$$

where $\sigma_{xb}$ is the extrusion pressure equation in each slab.

One of the extrusion die profiles that was designed in this research was done for commercially pure aluminum (AA1050). Hence to determine the *h* and $\sigma_0$ constants for this material, compression tests were carried out on a cylindrical sample with height to diameter ratio of 1.5 up to a strain value of 0.8. The obtained true stress-strain curve from this compression test is shown in Fig. 2. To determine the equation of the considered line, the linear regression of data with strains greater than 0.29 was used (Fig. 2). It is noteworthy that the trendline fitted to $\sigma-\varepsilon$ data has an R-square value equal to 0.993 that indicates the validity of equation fitted to data.

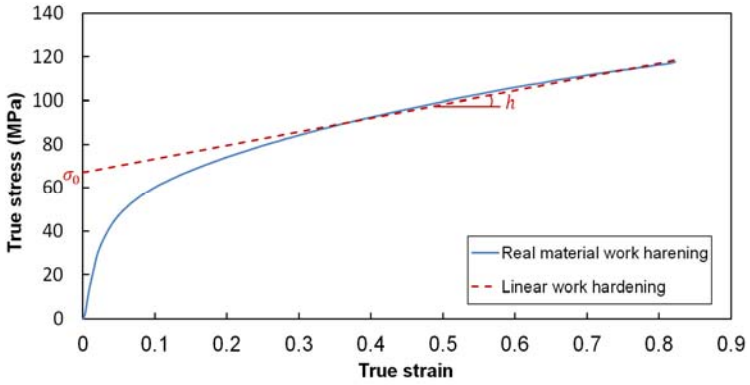


Fig. 2.True stress-strain curve of AA1050 alloy

***c) Redundant deformation***

If the deformation was ideal, plane sections of material would remain plane after deformation, but in practice, internal shear leads to distortion of plane sections during passing through deformation zone. Therefore, the material experienced a strain beyond what would be expected from considerations of homogenous deformation. Effect of this redundant work on the flow stress of material is analyzed by the redundant deformation factor $(\varphi)$. The magnitude of shear strain, generated due to redundant work, must be computed quantitatively and accurately. This is because of an increase in the total accumulated strain in the workpiece, which of course makes an increase in material work hardening and consequently causes an increase in required stress for extrusion of the metal through the die. Thus, it will have a dramatic effect on the optimal die profile.

To assess the value of this factor in each slab, an analytical method presented by Kazeminezhad [21] which was derived by upper bound theory is used. This proposed equation can be denoted as:

$$\varphi=1+\frac{\frac{\alpha}{\sin^2(\alpha)}-\cot\alpha}{\sqrt{3}f(\alpha)\ln(\frac{R_0}{R_f})} \tag{11}$$

Where $R_0$ and $R_f$ are the billet and extruded radiuses respectively and $f(\alpha)$ is a function of semi-die angle and is defined as:

$$f(\alpha)=\frac{1}{\sin^2(\alpha)}\left[1-\cos\alpha\sqrt{1-\frac{11}{12}\sin^2(\alpha)}+\frac{1}{\sqrt{132}}\ln\frac{1+\sqrt{\frac{11}{12}}}{\sqrt{\frac{11}{12}}\cos\alpha+\sqrt{1-\frac{11}{12}\sin^2(\alpha)}}\right] \quad (12)$$

It should be noted that the redundant deformation factor can also be measured by experimental methods. Superimposition of the true tensile stress-strain curves before and after deformation [22] and methods based on hardness measurements [23] are among the most important methods in this regard. However, using such methods for determining $\varphi$ will be comparatively sophisticated, costly and time-consuming. On the other hand, the analytical method utilized in the present investigation allows the value of $\varphi$ to be computed readily by using geometric characteristics of each slab.

***d) Iterative algorithm for minimization of extrusion pressure***

The algorithm reported by Noorani-Azad *et al.* [15] is utilized in this paper but it is improved to obtain a better mathematical representation for the die profile. This algorithm was implemented using MATLAB programming environment. The mentioned algorithm using an iterative procedure, generally by contemplating the bilateral effects of redundant work and friction in extrusion pressure and balancing between them, calculates the optimum angle and length of each slab. In other words, extrusion pressure in each slab is computed and compared for all semi-die angles from 0° to 90°. Then, based on this comparison, an optimum angle which results in minimum extrusion pressure is used as an optimum slab angle. Therefore, the coordinates of primary and ending points of each slab are determined after running the algorithm. The output of the iterative algorithm is a set of points which indicate the beginning and end of each slab on a 2-dimentional *r*-*x* plane. By fitting the points in a polynomial, the curved die profile is obtained. In the case of commercially pure aluminum as work metal, assuming a friction coefficient of 0.03 between tools and workpiece and area reduction of 75% the die profile equation is derived as:

$$r=-1.496\times10^{-7}x^6+9.791\times10^{-6}x^5-2.067\times10^{-4}x^4+0.001868x^3 -0.01944x^2+0.02391x+7.997 \quad (13)$$

It should be mentioned that the use of higher order polynomials for curve-fitting have an insignificant effect on the accuracy of fitted curve. The optimum die profile is depicted in Fig.3. It is seen that the resulted optimal die profile has continuous first derivatives at the die inlet and exit, causing the profile to be smoothly merged with the container at the inlet and with the die land at the exit. This feature aims to avoid any abrupt changes in velocity and cross section of flowing material while passing through deformation zone.

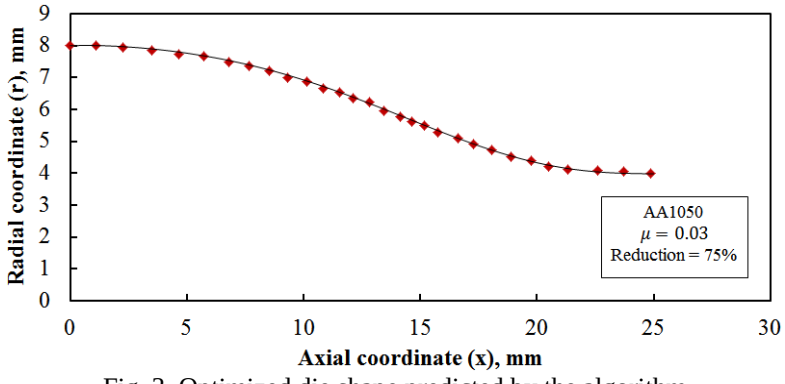


Fig. 3. Optimized die shape predicted by the algorithm

## 3. EXPERIMENTAL PROCEDURE

Commercially pure aluminum (AA1050) was used as a test material. Billets of 16 mm in diameter and 30 mm in length were machined out from an AA1050 thick sheet. The billets were annealed at $450\,°C$ for 2 h and then furnace cooled to room temperature. Teflon tape (PTFE) was used for lubrication. An appropriate die for 1050 Al with the die profile presented by Eq. 13 and also an optimum conical die was fabricated. The utilizing conical die has an optimum cone angle which is deduced using the following equation [24]:

$$\alpha_{opt} = \sqrt{\frac{3}{2} m \ln \frac{R_0}{R_f}} \tag{14}$$

For area reduction of 75% and friction factor of 0.1, the optimum angle would be 18 degrees.

Extrusion process through both optimum conical and curved die was carried out using a 200 kN screw press with ram speed of 0.2 mm/s at room temperature. The process was terminated at the steady state extrusion condition where the extrusion load and speed were maintained at constant levels. After the experiment, the partially extruded billets were removed from the extrusion apparatus to show the die profile as illustrated in Fig. 4.

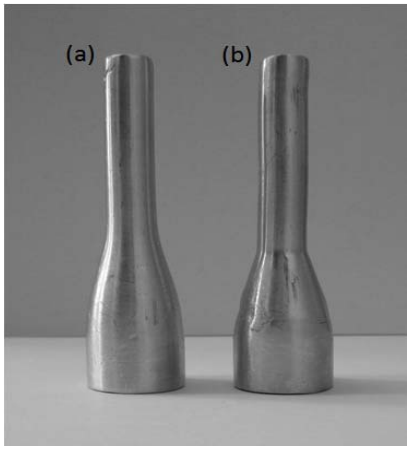


Fig. 4. Partially extruded products in different die profiles: (a) curved die, (b) conical die

Vickers microhardness tests were used for evaluation of mechanical property changes and its homogeneity. Samples were cut from each extruded product and measurements were done along the product diameters in two optionally perpendicular directions with an incremental step of approximately 0.5 mm. The hardness tests were performed by applying 100 gf load with rate of $5\,gs^{-1}$ and 15 s dwell time. Regarding the work hardening saturation in highly-deformed material, the hardness gradient cannot represent strain gradient. Hence, before performing the microhardness tests, specimens were partially annealed at $200\,°C$ for 20 minutes. This was done in order to supply the required energy for restoration phenomena and therefore transformation of cell structure walls into grain boundaries which results in much finer grain size. It is worth noting that the rate of increase in grain boundary density due to partial restoration is predominant over the dislocation annihilation at low temperature annealing, resulting in an increase in hardness.

## 4. FINITE ELEMENT ANALYSIS

To make a comparison with the developed curved die and to evaluate the effectiveness of the proposed approach, an optimal conical die was considered. Accordingly, the general purpose finite element code, ABAQUS/Explicit, was used to simulate and investigate characteristics of deformation in extrusion

process in both curved and conical dies. The curved die geometric model was built using CAD software and it was then imported to the FEM software. Due to the symmetrical characteristics of problem, two dimensional axisymmetric models were used for FE analyses. Geometric dimensions and mechanical properties of specimens in the simulation were the same as those of the experiment, making it possible to compare the simulation results with those obtained experimentally. A Young's modulus of 70 GPa and a Poisson's ratio of 0.33 were used for the material. The flow curve of material also was specified in section 2 as real material work hardening. In each case, the workpiece is discretized by means of 4-node bilinear axisymmetric quadrilateral, reduced integration with hourglass control elements (CAX4R). Reduced integration feature decreases the amount of CPU-time necessary for analysis of the model, and it typically provides more accurate results. The container, the die and the punch were considered as rigid bodies and hence did not require meshing. The die model is fully constrained by applying displacement boundary condition on its nodes, while the punch model is loaded by specifying displacement in the axial direction. The symmetrical boundary condition also imposed to the nodes of symmetry axis in order to arrest the displacement in the radial direction. The friction factor ($m$) at the die-sample interface was determined using barrel compression test [25]. Considering the lubrication condition, the value of 0.1 was obtained from this test. In order to apply this value in simulation, it was converted to friction coefficient $\mu = 0.03$ by using the following equation [26]:

$$\mu = \frac{m}{2\sqrt{3}} \tag{15}$$

By varying the number of elements, it was found that the 600 elements for initial deformable billet would be sufficient to obtain a reliable strain distribution and nearly mesh-independent solution. This is because the strain developed in the workpiece depends predominantly on mesh size [27]. The geometry of both curved and optimal conical die profiles are shown in Fig. 5(a) and (b) respectively, along with initial FE mesh used in the simulation (Fig. 5(c)).

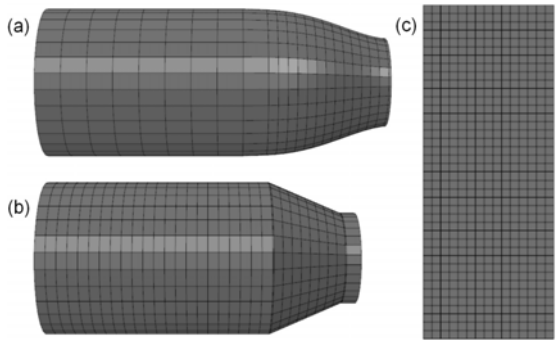


Fig. 5. (a) Configuration of curved die profile. (b) Configuration of conical die profile. (c) Initial mesh of the billet for FEA study

## 5. RESULTS AND DISCUSSIONS

### *a) Effect of work hardening characteristics and friction on the optimum die profile*

Extrusion ratio ($R$), friction coefficient ($\mu$) and material work hardening characteristics ($h$ and $\sigma_0$) are the input data to the algorithm and changing each of them could change the predicted optimum die profile. Here, the effects of work hardening and friction coefficient on the optimum die shape are investigated. In Fig. 6 the effect of material work hardening characteristics on the optimum die profile have been demonstrated by running the program for three different materials under the same extrusion ratio and friction coefficient. AA1050, stainless steel and electrolytic copper are the three investigated materials and

work hardening characteristics of these materials are given in Table 1. Determination of $h$ and $\sigma_0$ for stainless steel was done based on the constitutive equation published in [28].

Table 1. Work hardening characteristics of the three considered materials

| Work hardening characteristics | AA1050 | Stainless steel [a] | Electrolytic copper [b] |
|---|---|---|---|
| $\sigma_0$ (MPa) | 67.3 | 297.4 | 338.0 |
| $h$(MPa) | 62.9 | 349.8 | 132.9 |

[a] AISI 321H.
[b]Ref. [16].

By increasing work-hardenability of material, i.e. increasing "$h$" in the linear work hardening model, the length of die will increase as shown in Fig. 6. This finding is consistent with the results of Byon and Hwang [5] who investigated the effects of taking into account the material strain hardening on die profile via FEM. The reason for this phenomenon is that increasing the work-hardenability of a material is equivalent to increasing the sensitivity of its flow stress with respect to the imposed strain. Hence, in such conditions, the workpiece would be more susceptible to increase in its flow stress by developing a small strain. Thus, redundancy becomes the dominant factor in comparison to frictional effect in increasing extrusion pressure, causing the optimum cone angle of each slab to be reduced to minimize the redundancy effect. This leads to an increase in the die length.

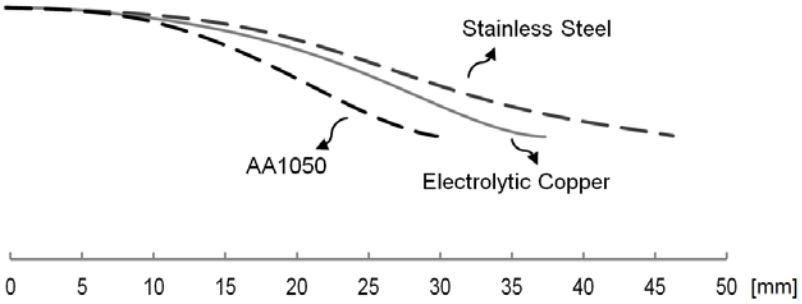


Fig. 6. Effect of material work hardening characteristics on the optimum die profile ( $\mu$ = 0.03)

Increasing friction coefficient in the die-workpiece interface, however, causes a decrease in optimal die length as illustrated in Fig. 7. The reason why this happens is that friction effect becomes a prevailing factor compared to the redundant effect. This occurs by increasing the optimum semi-die angle of each slab.

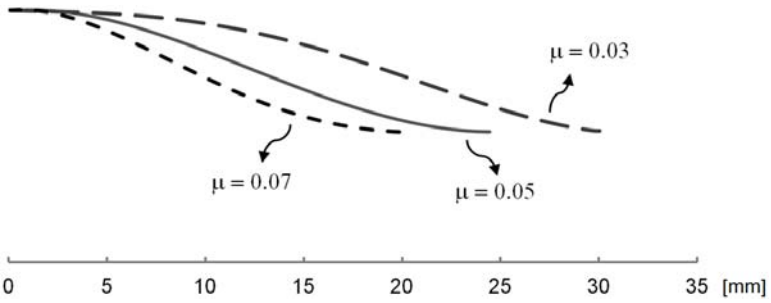


Fig. 7. Effect of friction on the optimum die profile (AA1050)

***b) Load requirement***

Fig. 8 illustrates the load-displacement curves for extrusion process through proposed curved die and optimum conical die which are obtained both experimentally and numerically. It can be seen that a lower

load is required for extrusion process using the designed curved die in comparison with optimum conical die. At first glance, the reduction in maximum load may appear as inconsiderable. However, when one extrudes higher strength alloys like high alloy steels this reduction becomes significant. This is due to the fact that the redundant work occurs in the process is linearly dependent to shear strength of workpiece. Also, it is observed that there is an acceptable agreement between experimental and simulated load curves; the error between the two methods in the peak point for conical and curved die is 1.70% and 1.36% respectively. Thus, it confirms the validity of the results obtained by simulation.

The load-displacement curves obtained from the FEM analysis were first smoothened using Butterworth filter, implemented in ABAQUS software, in order to reduce the undesirable high frequency fluctuations in the data. These fluctuations are due to repeated contacting and separating of nodes of the billet with the die surface. In other words, as the billet exits the die, its contact nodes are released. This causes a drop in the required extrusion force. As the material continues to enter the die, another contact node reaches the exit point of the die resulting in increase of the extrusion force. This condition can be attributed to the FE nature in which the nodes that are released as the billet exits the die are a finite distance apart, consequently resulting in the above-mentioned fluctuations in extrusion pressure. The problem of oscillation in the load-displacement curve can be alleviated alternatively by making the contact elements so small.

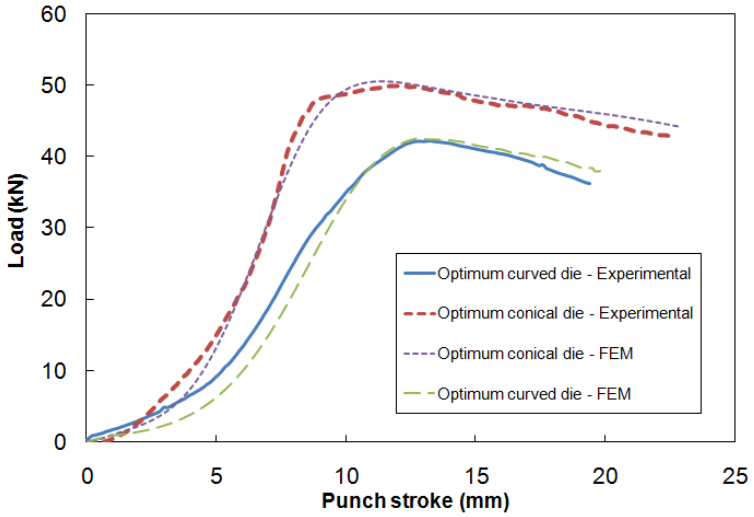


Fig. 8. Load-displacement curves obtained by the experiment and simulation for extrusion process through conical die and curved die ( $\mu$ = 0.03, $R$= 2:1)

Figure 8 also shows that at the early stage of deformation, the material has not yet filled up the cavity of the die completely and unsteady state deformation occurs. As a result, the required load initially increases until it attains a peak value, then it drops and reaches a steady value as the deformation progresses. The gradual decrease in the load–displacement curves is owing to decreasing the frictional surface area in the container as the punch advances.

### *c) Strain homogeneity*

One of the major advantages of the proposed curved die compared to conical die is the uniformity of strain distribution in the cross section of the extrusion product.

The redundant strain experienced by the material in a non-optimal extrusion die makes the microstructure of the extruded product demonstrate some steep changes in the cross section. The microstructure heterogeneity leads to the non-uniform mechanical properties in the extruded material [29], and also may adversely affect the corrosion behavior of the material [30]. To deliberate this strain

inhomogeneity, distribution of plastic strain in product is considered. Fig. 9 illustrates this strain distribution in the cross section of the processed specimens which extruded through both optimum conical and curved die. As can be seen in this figure, strain distribution in the sample extruded by curved die is more uniform. Consequently, it is expected that an acceptable homogeneity in the mechanical properties of this product will be developed. Also, it is quantitatively obvious that the strain values are lower in the final product extruded through curved die. This can be explained by considering the more redundant strain experienced by the material during extrusion through conical die. It should be noticed that the horizontal axis of Fig. 9 is normalized by workpiece diameter.

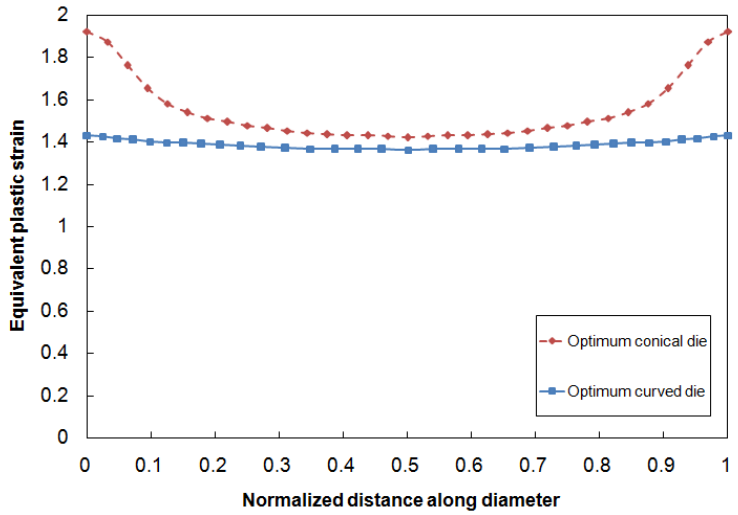


Fig. 9. Comparison of plastic strain distribution at the cross section of the product

Deformation homogeneity was also evaluated experimentally via Vickers microhardness test. Fig. 10 represents microhardness profile on the cross section of the processed samples which were annealed subsequently. As it can be seen, a very good homogeneity of microhardness is presented across the samples processed by curved die despite what is seen in the sample processed by conical die. This distribution of hardness provides good compatibility with strain distribution shown in Fig. 9.

It is worthwhile to note that extrusion through non-optimal conical dies and lower reduction percentages will amplify deformation inhomogeneity in processed product.

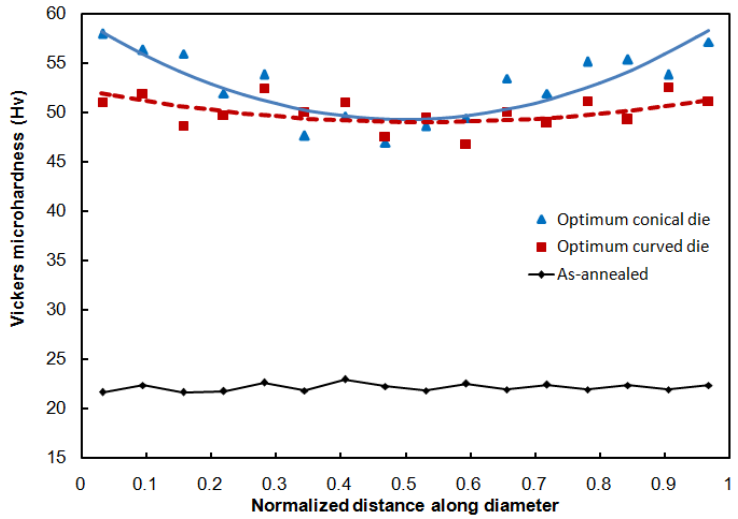


Fig. 10. Hardness evolutions across the products diameter

### *d) Grid distortion pattern*

A powerful tool for studying the flow pattern is plotting the grid distortion of the workpiece after deformation. Understanding and predicting metal flow during extrusion is crucial as metal flow dictates the velocity and strain gradients experience, largely influencing final microstructure and properties of the final product. Therefore, to observe the material flow during the process, grid deformation patterns in longitudinal section of workpiece were studied using FE simulation. Fig. 11 compares the flow patterns of the two kinds of dies studied in the present work. The arrows on the figure are an indicator of flections measure of grid lines and give a sense of distortion magnitude. Comparing these patterns, one observes that the conical die causes greater grid distortions compared to curved die. This explains why the material needs a lower load to be extruding through optimum curved die.

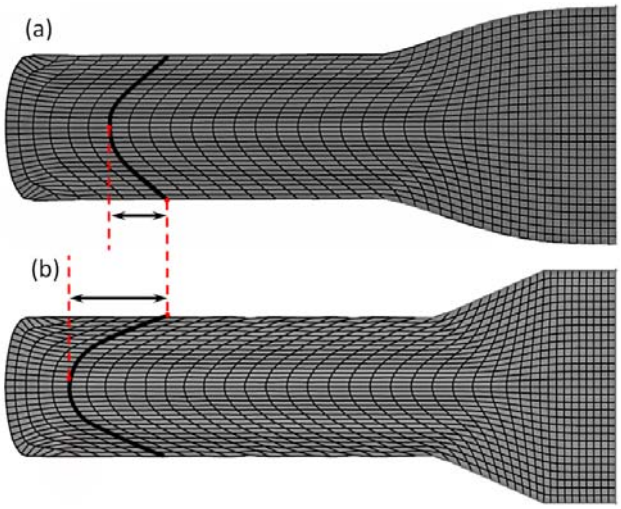


Fig. 11. Grid distortion patterns for two kind of dies: (a) curved die (b) conical die ( $\mu$ = 0.03)

### *e) Wear behavior*

The service life of die is an important factor in the productivity and cost effectiveness of the extrusion process however it is always limited by wear. Cold extrusion dies may require frequent replacement due to the high level of wear that leads to poor surface quality, loss of dimensional accuracy and die failure.

The theories of wear can be classified according to the contacting conditions. Amongst the wear theories, the abrasive wear theory is generally applied to the wear mechanism in cold forming processes. In extrusion process also, abrasive wear mechanism is the dominant wear mechanism [31]. Archard [32] introduced a model for the wear phenomenon, proposing that the wear phenomenon is the collapse of micro-asperities on the two contacting bodies. The amount of wear according to this model is linearly proportional to normal stress. Accordingly, minimization of the normal stress at tool-workpiece interface will minimize the level of wear in die and improve its life [33].

To compare the wear behavior in both curved die and conical die, normal stress distribution along die-workpiece interface is investigated using FE results. For the same extrusion conditions of Fig. 11, Fig. 12 demonstrates a comparison between the optimum conical and optimum curved die profiles regarding the normal stress acting on the die along the tool–workpiece interface. It should be realized that the horizontal axis of Fig. 12 is normalized by contact length of workpiece and die in the deformation zone. As seen in this figure, stress developed at the interface is quite lower and more uniformly distributed in the case of optimal curved die. Thus, based on Archard's model it is expected that the die life of optimal curved die profile be longer than that of the optimal conical die.

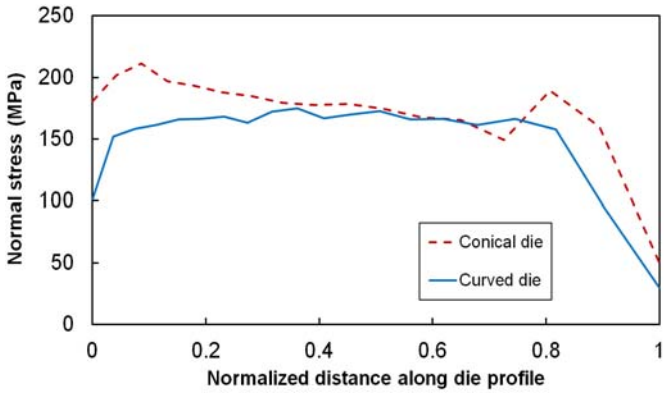


Fig. 12. Comparison of normal stress along die-interface for conical and curved dies

## 6. CONCLUSION

In the present study, extrusion die profile is optimized based on an improved slab analysis. To evaluate the algorithm efficiency, the extrusion process through both optimum conical and curved die was performed experimentally and analyzed by finite element method. The following conclusions can be drawn from this investigation:

1. The proposed approach can be a simple and yet efficient tool for an optimum design of die profile.
2. Material work hardening characteristic and friction condition have significant effect on the optimal die shape.
3. The designed die can be used to produce desirable conditions in both process and product quality in terms of extrusion force, deformation homogeneity and die wear.

## REFERENCES

1. Richmond, O. & Devenpeck, M. L. (1962). A die profile for maximum efficiency in strip Drawing. ASME, Proc 4th U S National Congress Applied Mechanic, 1053-1057.
2. Srinivasan, R., Gunasekera, J. S., Gegel, H. L. & Doraivelu, S. M. (1990). Extrusion through controlled rate dies. *Journal of Materials Shaping Technology*, Vol. 8, pp. 133-141.
3. Lu, Y. H. & Lo, S. W. (1999). An advanced model of designing controlled strain rate dies for axisymmetric extrusion. *Journal of Materials Engineering Perform*, Vol. 8, pp. 51–60.
4. Jooybari, M. B., Saboori, M., Azad, M. N. & Hosseinipour, S. J. (2007). Combined upper bound and slab method, finite element and experimental study of optimal die profile in extrusion. *Materials and Design*, Vol. 28, pp. 1812-1818.
5. Byon, S. M. & Hwang, S. M. (2003). Die shape optimal design in cold and hot extrusion. *Journal of Materials Processing Technology*, Vol. 138, pp. 316-324.
6. Lin, Juchen X., Xinyun, W. & Guoan, H. (2003). Optimization of die profile for improving die life in the hot extrusion process. *Journal of Materials Processing Technology*, Vol. 142, pp. 659-664.
7. Kim, N. H., Kang, C. G. & Kim, B. M. (2001). Die design optimization for axisymmetric hot extrusion of metal matrix composites. *International Journal of Mechanical Science*, Vol. 43, pp. 1507-1520.
8. Gordon, W. A., Van Tyne, C. J. & Moon, Y. H. (2007). Axisymmetric extrusion through adaptable dies—Part 1: Flexible velocity fields and power terms. *International Journal of Mechanical Science*, Vol. 49, pp. 86-95.
9. WA, Van Tyne C. J. & Moon, Y. H. (2007). Axisymmetric extrusion through adaptable dies—Part 2: Comparison of velocity fields. *International Journal of Mechanical Science*, Vol. 49, pp. 96-103.
10. Gordon, W. A., Van Tyne, C. J. & Moon, Y. H. (2007). Axisymmetric extrusion through adaptable dies—Part 3: minimum pressure streamlined die shapes. *International Journal of Mechanical Science*, Vol. 49, 104-115.

11. Yang, D. Y. & Han, C. H. (1987). A new formulation of generalized velocity field for axisymmetric forward extrusion through arbitrarily curved dies. Trans ASME, *Journal of Engineering Industry*, Vol. 109, pp. 161-168.
12. Ponalagusamy, R., Narayanasamy, R. & Srinivasan, P. (2005). Design and development of streamlined extrusion dies: A Bezier curve approach. *Journal of Materials Processing Technology*, Vol. 161, pp. 375-380.
13. Pahlavani, Z. & Ebrahimi, R. (2013). Optimization of specific die profiles in thin walled tube extrusion. *Iranian Journal of Science and Technology, Transactions of Mechanical Engineering*, Vol. 37, No. M2, pp. 203-215.
14. Wifi, A. S., Shatla, M. N. & Abdel Hamid, A. (1998). An optimum-curved die profile for hot rod extrusion process. *Journal of Materials Processing Technology*, Vol. 73, pp. 97-107.
15. Noorani-Azad, M., Bakhshi-Jooybari, M., Hosseinipour, S. J. & Gorji, A. (2005). Experimental and numerical study of optimal die profile in cold forward rod extrusion of aluminum. *Journal of Materials Processing Technology*, Vols. 164-165, pp. 1572-1577.
16. Panteghini, A. & Genna, F. (2010). An engineering analytical approach to the design of cold wire drawing processes for strain-hardening materials. *Internatinal Journal of Materials Forming*, Vol. 3, pp. 279-289.
17. Sachs, G. (1927). Beitrag zur Theorie des Ziehvorganges. *Z Angew Math Mech*, Vol. 7, pp. 235-236.
18. Hosford, W. F. & Caddell, R. M. (1993). *Metal forming: Mechanics and metallurgy*. Third ed., Prentice Hal, Englewoodcliffs.
19. Panteghini, A. & Genna, F. (2010). Effects of the strain-hardening law in the numerical simulation of wire drawing processes. *Computational Materials Science*, Vol. 49, pp. 236–242.
20. Verlinden, B., Driver, J., Samajdar, I. & Doherty, R. D. (2007). *Thermo-Mechanical processing of metallic materials*. Pergamon Materials Series, Elsevier, Amsterdam.
21. Kazeminezhad, M. (2008). A study on the computation of the redundant deformation factor in wire drawing of austenitic 304 stainless steel. *Journal of Materials Processing Technology*, Vol. 199, pp. 230-233.
22. Caddell, R. M. & Atkins, A. G. (1968). The influence of redundant work when drawing rods through conical dies. Trans ASME B, *Journal of Engineering Industry*, Vol. 90, pp. 411-419.
23. Backofen, W. A. (1972). *Deformation processing*. Addison-Wesley, Massachusetts.
24. Avitzur, B. (1968). *Metal forming: Processes and analysis*. McGraw-Hill, New York.
25. Ebrahimi, R. & Najafizadeh, A. (2004). A new method for evaluation of friction in bulk metal forming. *Journal of Materials Processing Technology*, Vol. 152, pp. 136-143.
26. Rao, K. P. & Sivaram, K. (1993). A review of ring-compression testing and applicability of the calibration curves. *Journal of Materials Processing Technology*, Vol. 37, pp. 295-318.
27. Inoue, T. & Tsuji, N. (2009). Quantification of strain in accumulative roll-bonding under unlubricated condition by finite element analysis. *Computational Materials Science*, Vol. 46, pp. 261-266.
28. Yuan, S. J., Han, C. & Wang, X. S. (2006). Hydroforming of automotive structural components with rectangular sections. *International Journal of Machine Tools Manufacturing*, Vol. 46, pp. 1201-1206.
29. Kaneko, S., Murakami, K. & Sakai, T. (2009). Effect of the extrusion conditions on microstructure evolution of the extruded Al–Mg–Si–Cu alloy rods. *Materials Science Engineering A*, Vol. 500, pp. 8-15.
30. Minoda, T. & Yoshida, H. (2002). Effect of grain boundary characteristics on intergranular corrosion resistance of 6061 aluminum alloy extrusion. *Metallurgical Materials Transaction A*, Vol. 33A, pp. 2891-2898.
31. Lepadatu, D., Hambli, R., Kobi, A. & Barreau, A. (2006). Statistical investigation of die wear in metal extrusion process. *International Journal of Advanced Manufacturing Technology*, Vol. 28, pp. 272-278.
32. Archard, J. F. (1953). Contact and rubbing of flat surfaces. *Journal of Applied Physics*, Vol. 24, pp. 981-988.
33. Lee, G. A. & Im, Y. T. (1999). Finite-element investigation of the wear and elastic deformation of dies in metal forming. *Journal of Materials Processing Technology*, Vols. 89–90, pp. 123-127.